MECSOL 2022 - Proceedings of the 8th International Symposium on Solid Mechanics
M.L. Bittencourt, J. Labaki, L.C.M. Vieira Jr. and E. Mesquita (Editors), Campinas SP, Brazil, October 17th to 19th, 2022

Investigation of geometrical properties of single-phase local resonators in the formation of bandgaps in three-dimensional elastic metamaterials

Ana Carolina Azevedo Vasconcelos[1] and Jovana Jovanova[1]

[1] Faculty of Mechanical, Maritime and Materials Engineering, Delft University of Technology, Mekelweg 2, 2628 CD Delft, The Netherlands

Abstract: Elastic metamaterials – man-made resonant structures exhibiting unusual functionalities – have shown promising results for controlling structural vibration, specially at a low frequency regime. Such functionalities rely on the presence of resonant bandgaps, which consists of a frequency band where waves cannot propagate in response to the out-of-phase motion of the local resonators. Usually, the contrast between the properties of different material phases in such resonators results on the resonant effect, however, the manufacturing of such multi-phase structures is challenging and can be a high-cost process. This work proposes a parametric investigation of an elastic metamaterial constituted by single-phase local resonators. The bandgap formation in such structure depends on the geometrical properties of the resonators, instead of the material parameters. This analysis allows us to understand which geometrical features are sensitive to the position of the resonant bandgaps and its width. Designing such single-phase resonators provides an alternative to manufacture low-cost structures for engineering application.
Keywords: locally resonant bandgap, single-phase resonator, elastic metamaterial

INTRODUCTION

The extensive studies in acoustic/elastic metamaterials (A/E MMs) have highlight their feasibility in reducing low-frequency noise/vibration, which emerged to overcome the limitation of phononic crystals (PnCs) with respect to their wave control mechanism. Different from PnCs, which rely on their lattice size to create the destructive interference between waves, A/E MMs relies on the formation of subwavelength bandgaps – frequency regions where waves cannot propagate – due to the presence of periodically arranged internal resonators. In the local resonance (LR) mechanism, the energy of the incident wave is absorbed at the resonant frequency of the unit cell, which prevents the wave transmission through the domain. The first concept of a LR metamaterial was reported by Liu et al. (2000), in which they obtained negative elastic parameters at specific frequencies by using a unit cell containing a stiff core material covered by a soft material. Mass-spring systems realize negative mass density when the resonator moves out-of-phase with the income wave (Milton and Willis, 2007). This phenomenon has been named as dipolar resonance. Researchers have investigated variations of mass-spring systems, such as dual-resonator system (Tan, Huang and Sun, 2014), cantilever-in-mass metamaterials (Qureshi, Li and Tan, 2016) and mass-spring systems to reach negative Young's modulus (Huang and Sun, 2011).

The resonant bandgap has been reached by the combination of two or more materials, so that the core of the resonator is formed by a stiffer material while the coating is made of a soft material. An acoustic MM formed by rubber-coated gold spheres immersed in epoxy was designed to achieve simultaneously negative mass density and modulus (Deng et al., 2009). Popa and Cummer (2014) proposed a metamaterail-based structure formed by Helmholtz resonators that provide specific behaviors for different directions of wave propagation. Although this is a straightforward strategy to guarantee a resonant phenomenon, manufacturing resonators with discontinuous distribution of material properties can require complex processes (Bandyopadhyay and Heer, 2018).

Single-phase resonant unit cells have been investigated to address the issue regarding to the manufacturing complexity. The topology of such structures usually consists of holes with a certain profile that can generate the resonance phenomenon. Such profiles can also be fabricated by using cutting techniques, which is a low-cost and less complex process. Gao et al. (2019) theoretically designed a single-phase platonic crystal, a type of metamaterial-based thin plate. The resonator of such crystal is made of beam-type structures distributed over a cavity. The geometrical parameters of the beam and the cavity are strictly related to the resonance of the system. Various numerical examples of single-phase metamaterials have also been reported. Sang, Sandgren and Wang (2018) explored analytically and numerically the influence of translational and rotational resonances in periodic chiral local resonators. They noticed that the translational resonator was responsible for obtaining negative effective mass density, whereas the rotational resonance leads to negative effec-

tive modulus. The combination of both resonances resulted in double-negative effective material properties. Warmuth, Wormser and Körner (2017) proposed a single-phase phononic crystal which reproduces the dynamic characteristic of a dual phase crystal by combining soft and stiff struts. For the first time, they experimentally exhibited the predicted band gaps. Jiang et al (2021) explored a single-phase structure that generates both Bragg scattering and locally resonant band gaps. They also fabricated the metamaterial by using additive manufacturing and validated experimentally the numerical results. Due to the reduction in the design parameters, especially the ones related to the materials properties, optimization techniques have been applied to design the single-phase A/E MMs. Genetic Algorithm (GA) has been employed by Dong et al. (2018) to design single-phase metallic structures to achieve super resolution imaging. Lin et al. (2021) used shape optimization to achieve the design of double negativity of chiral elastic MMs.

In view of the advanced studies in single-phase A/E MMs, we evaluate the influence of the resonator's components in the bandgap formation. The analysis is restricted to the in-plane geometric parameters that are strictly related to the mass and stiffness of the resonator. We identify which geometric parameter is more sensitive to change the bandgap with respect to its bandwidth and its central frequency. The findings of this work contribute to design the bandgap of single-phase A/E MMs for applications extending from low to high frequency waves.

MODEL DESCRIPTION

The single-phase unit cell proposed in this paper consists of a cylindrical resonator attached to an external frame through four identical beams as shown in Fig. 1. Introducing the beam's length inside the resonator is proposed to modify the resonant bandgap with respect to this dimension, while holding the size of the unit cell fixed. The depth of the entire structure is kept constant so that the resonant effect is evaluated by using the in-plane dimensions. The geometric parameters defining the topology of the unit cell are presented in Tab. 1. The constitutive material of the unit cell is nylon, whose material properties are Young's modulus E = 2 GPa, density ρ = 1050 kg/m^3 and Poisson's ratio ν = 0.33. No damping is considered in the model. Due to the symmetry of the unit cell in both in-plane directions, its smallest periodic component is represented by the green triangle $\Gamma - X - M - \Gamma$, as indicated in Fig. 1. Such region, which is also named as the Irreducible Brillouin Zone (IBZ), can be used to predict the dynamic characteristics of the unit cell.

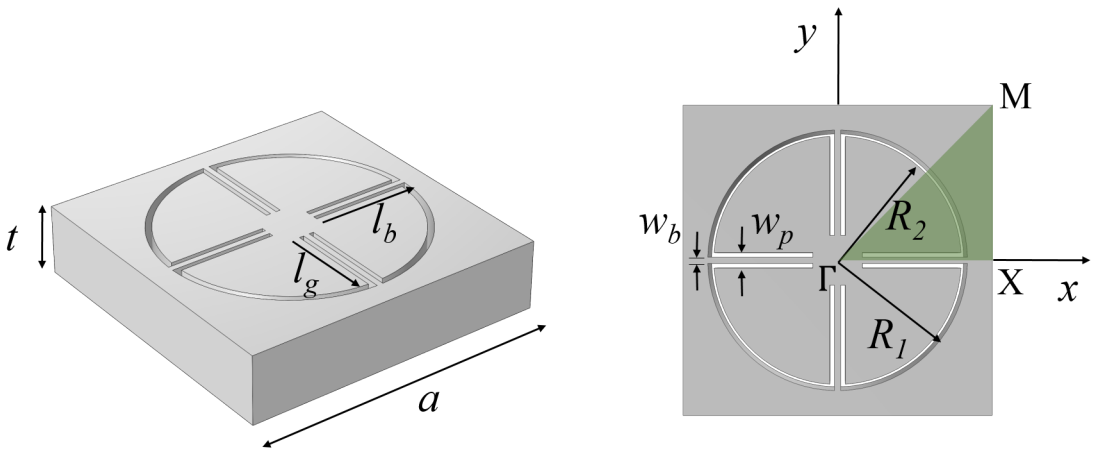

Figure 1 – Single-phase unit cell and its geometric parameters. The green triangle represents the Irreducible Brillouin Zone (IBZ), which defines the smallest periodic component of the unit cell.

METHODS

The resonant bandgap is evaluated by obtaining the dispersion relation and the effective mass density of the unit cell. For the former method, the wave propagation problem in an infinite periodic medium can be evaluated by enforcing periodic boundary conditions are enforced at the unit cell's edges through the following Bloch-Floquet relation,

$$\mathbf{u}(\mathbf{x}+\mathbf{r}) = \mathbf{u}(\mathbf{x})e^{i(\mathbf{k}\cdot\mathbf{r}-\omega t)}, \tag{1}$$

Table 1 – Definition of the geometric parameters of the unit cell.

variable	Description	Variable	Description
a	Unit cell size	w_p	Width of the beam's path
R_1	Radius of cavity	l_p	Depth of the beam's path
R_2	Radius of resonator	w_b	Width of the beam
t	Unit cell thickness	l_b	Length of the beam

where $\mathbf{u}$ is the displacement field, $\mathbf{x}$ is the position vector, $\mathbf{r}$ is the spatial periodicity, ω is the frequency, and $\mathbf{k} = k_x i + k_y j$ is the wave vector. The following eigenvalue problem is defined as

$$(\mathbf{K} - \omega^2 \mathbf{M})\Phi = \mathbf{0}, \tag{2}$$

where $\mathbf{K}$ and $\mathbf{M}$ are the stiffness and mass matrices, respectively, and Φ is the eigenvector describing the wave modes of the unit cell. Eq. 2 is solved by assigning a set of predefined wavevectors in the edges of the IBZ and then obtaining the frequencies ω. Such edges are identified as the path $\Gamma(0,0,0) - X(\pi/a,0,0) - M(\pi/a,\pi/a,0) - \Gamma(0,0,0)$. The obtained frequencies are normalized with respect to the unit cell size a, and the longitudinal wave speed c_l, which is the square root of the ratio between the Young's modulus E and the density ρ.

The latter method consists of calculating the effective mass density of the unit cell, which is performed by exciting the unit cell external boundaries with a harmonic force and evaluating its frequency response through solving the system (Lai et al, 2011),

$$(\mathbf{K} - \omega^2 \mathbf{M})\mathbf{u} = \mathbf{f}, \tag{3}$$

where $\mathbf{u}$ and $\mathbf{f}$ represent the external force and displacement vectors. Therefore, the effective mass density is obtained by calculating the average of the external loads with the acceleration on the unit cell boundaries as,

$$\rho_{eff}(\omega) = -\frac{1}{V}\frac{|\mathbf{f_b}|}{\omega^2 |\mathbf{u_b}|}, \tag{4}$$

where V is the volume of the unit cell, and $\mathbf{f_b}$ and $\mathbf{u_b}$ are the force and displacement evaluated at the external boundaries of the unit cell, respectively. The influence of the geometric properties of the resonator on the bandgap formation is evaluated in three case studies: varying the beam dimensions w_b and l_b, and the radius of the cylindrical mass R_2. The width and the central frequency of the bandgaps are obtained for each dimension.

RESULTS

As a reference example for the study of the geometric properties of the resonator, a single-phase unit cell with parameters $R_1 = 0.42a, R_2 = 0.4a, w_b = 0.02a, l_g = 0.08a, w_g = 0.05a$, and $t = 0.23a$ is investigated. Fig. 2 presents the dispersion diagram and the effective mass density for such unit cell. A complete bandgap is observed at the frequency range extending from the nondimensional frequency Ω = 0.051 to Ω = 0.056 (shaded area). The flat shape of the lower band is an indicative that this bandgap is formed by the resonance of the unit cell. The effective mass density curve also indicates the presence of a bandgap at the region with a negative value of the ratio ρ_{eff}/ρ_{nylon}. In this region, the resonator has an out-of-phase motion in relation to the host medium (Milton and Willis, 2007). Notice a slight difference between the position of both shaded areas, due to the calculation of the effective mass density requires a finite structure, while an infinite periodic medium was assumed to evaluate the dispersion relation.

Figure 3 presents the bandgap variation with the increase of the three geometric parameters of the resonator. The red curve and black curve represent, respectively, the upper and lower bound of the bandgap. The central frequency is illustrated by the blue curve, while the bandwidth is highlighted by the shaded area. In the first case study, the beam's width varies from 0.004 m to 0.01 m, while the other dimensions remain the same. Notice that the increase in w_b results in the enlargement of the bandgap and the increase of the central frequency value. On the other hand, the increase of the beam's length and the resonator's radius causes the decrease of the central frequency. For such cases, the beam's length varies from 0.128 m to 0.138 m, while the mass' radius extends from 0.14 m to 0.16 m. The upper bound of the bandgap decreases suddenly for $l_b = 0.135$ m, which we notice a reduction in the bandwidth of the bandgap. For lower values of l_b and R_2, the bounds overlap each other, which means that there is no bandgap at such dimensions. For these studies, we notice that the bandgap properties is related to the resonant mechanism of the unit cell, which means that increasing the beam's width results in the increase of the stiffness of the resonator. Consequently, the resonance frequency will increase

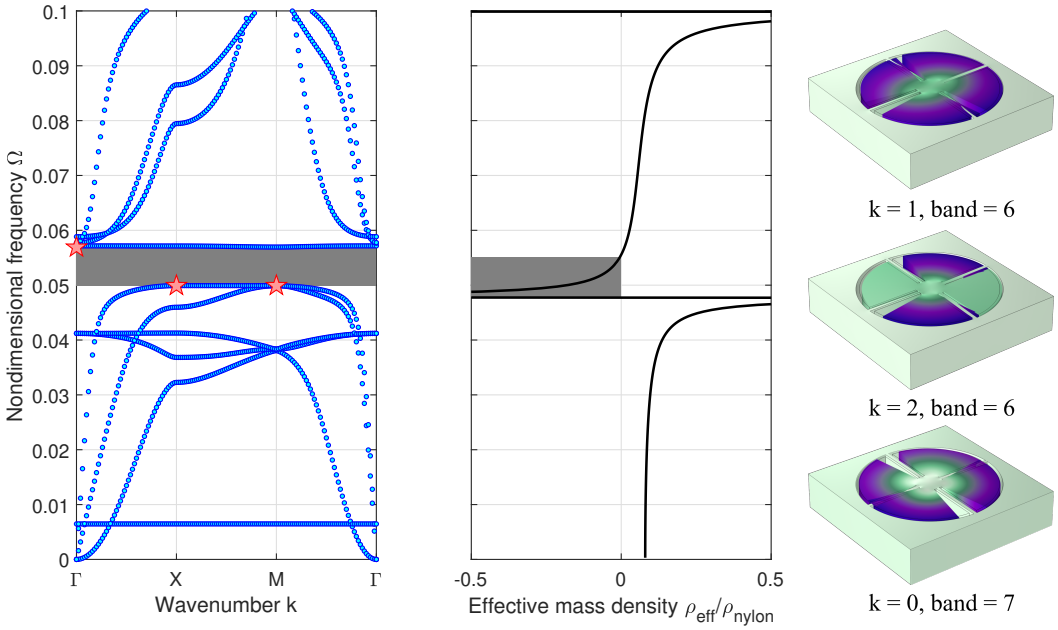

Figure 2 – Dispersion relation (left) and effective mass density (center) of the single-phase unit cell presented in Fig. 1. The shaded area represents a complete bandgap. (right) Modes before and after the bandgap highlighted by the pentagram markers.

and the central frequency of the bandgap will be higher. Similarly, increasing the beam's length or the mass' radius cause the reduction of the unit cell's stiffness, which drives the central frequency of the bandgap to lower levels.

CONCLUSIONS

In this paper, we presented the effect of the geometric parameters of the resonator on the bandgap formation. The analysis was performed in the main components of the resonator, which are the width and the length of the beams and the radius of the resonator. Since the unit cell is constituted of a single material, a nondimensional frequency was defined to remove the dependency on the material properties, so that the geometric parameters of the resonator are investigated separately. The case studies showed that the bandgap position is related to the resonant properties of the unit cell, which are intrinsically dependent of the beams and mass dimensions. Also, we observed that increasing the beam's length without modifying the size of the unit cell guarantees the reduction of the central frequency of the bandgap. Performing parametric studies in the resonator's components enables designing unit cells for applications ranging from low to high frequency wave attenuation.

ACKNOWLEDGMENTS

The authors would like to thank Delft University of Technology for enabling this research as cohesion project awarded by the faculty of Mechanical, Maritime and Materials Engineering.

REFERENCES

Bandyopadhyay, A. and Heer, B., 2018, "Additive manufacturing of multi-material structures", Materials Science and Engineering: R: Reports, Vol. 129, pp. 1-16.

Deng, K., Ding, Y., He, Z., Zhao, H., Shi, J. and Liu, Z., 2009, "Theoretical study of subwavelength imaging by acoustic metamaterial slabs", Journal of Applied Physics, Vol. 105, n. 12.

Dong, H. W., Zhao, S. D., Wang, Y. S. and Zhang, C., 2018, "Broadband single-phase hyperbolic elastic metamaterials for super-resolution imaging", Scientific reports, Vol. 8, n. 1, pp. 1-10.

Gao, P., Climente, A., Sánchez-Dehesa, J. and Wu, L., 2019, "Single-phase metamaterial plates for broadband vibration

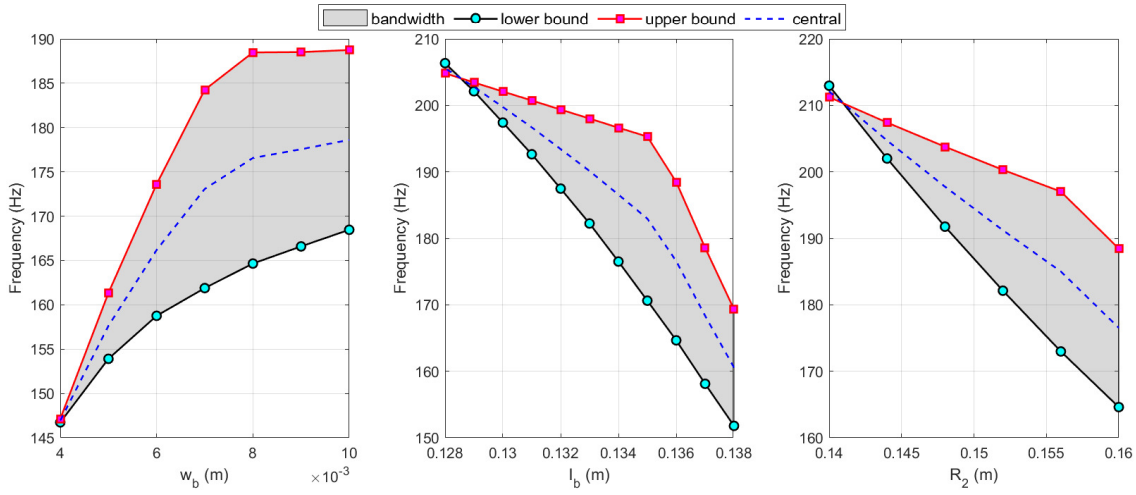

Figure 3 – Bandgap variation with alteration of the main geometric parameters of the resonator.

suppression at low frequencies", Journal of Sound and Vibration, Vol. 444, pp. 108-126.

Huang, H. H. and Sun, C. T., 2011, "Theoretical investigation of the behavior of an acoustic metamaterial with extreme Young's modulus", Journal of the Mechanics and Physics of Solids, Vol. 59, n. 10, pp. 2070-2081.

Jiang, W., Yin, M., Liao, Q., Xie, L. and Yin, G., 2021, "Three-dimensional single-phase elastic metamaterial for low-frequency and broadband vibration mitigation", International Journal of Mechanical Sciences, Vol. 190.

Lai, Y., Wu, Y., Sheng, P. and Zhang, Z. Q, 2011, "Hybrid elastic solids", Nature materials, Vol. 10, n. 8, pp. 620-624.

Lin, X. Y., Li, E., He, Z. C., Wu, Y. and Li, Q. Q, 2021, "Design of single-phase chiral metamaterials for broadband double negativity via shape optimization", Applied Mathematical Modelling, Vol. 91, pp. 335-357.

Liu, Z., Zhang, X., Mao, Y., Zhu, Y. Y., Yang, Z., Chan, C. T. and Sheng, P., 2000, "Locally resonant sonic materials", Science, Vol. 289, n. 5485, pp. 1734-1736.

Milton, G.W. and Willis, J.R., 2007, "On modifications of Newton's second law and linear continuum elastodynamics", Proceedings of the Royal Society A: Mathematical, Physical and Engineering Sciences, Vol. 463, n. 2079, pp. 855-880.

Popa, B. I. and Cummer, S. A., 2014, "Non-reciprocal and highly nonlinear active acoustic metamaterials", Nature communications, Vol. 5, n. 1, pp. 1-5.

Qureshi, A., Li, B. and Tan, K. T., 2016, "Numerical investigation of band gaps in 3D printed cantilever-in-mass metamaterials", Scientific reports, Vol. 6, n. 1, pp. 1-10.

Sang, S., Sandgren, E. and Wang, Z., 2018, "Wave attenuation and negative refraction of elastic waves in a single-phase elastic metamaterial", Acta Mechanica, Vol. 229 , n. 6, pp. 2561-2569.

Tan, K. T., Huang, H. H. and Sun, C. T., 2014, "Blast-wave impact mitigation using negative effective mass density concept of elastic metamaterials", International Journal of Impact Engineering, Vol. 64, pp. 20-29.

Warmuth, F., Wormser, M. and Körner, C., 2017, "Single phase 3D phononic band gap material", Scientific reports, Vol. 7, n. 1, pp. 1-7.

RESPONSIBILITY NOTICE

The author(s) is (are) the only party(ies) responsible for the printed material included in this paper.